JOURNAL OF MATERIALS SCIENCE 28 (1993) 3911–3922

Chemical stability of titanium diboride reinforcement in nickel aluminide matrices

J. D. RIGNEY, J. J. LEWANDOWSKI
Department of Materials Science and Engineering, The Case School of Engineering, Case Western Reserve University, Cleveland, OH 44106, USA

Chemical stability of titanium diboride (TiB_2) reinforcement in NiAl (45 at% Al) and Ni_3Al (24 at% Al) matrices has been theoretically and experimentally investigated. Calculations were made using thermodynamic properties of the systems to predict behaviour at temperatures between 1173 and 1573 K. Experimental investigation of hot-press consolidated TiB_2 particulate/prealloyed matrix powder blends were conducted using energy dispersive X-ray analysis, X-ray diffraction analysis, Auger electron spectroscopy and transmission electron microscopy. The theoretical and experimental analyses suggest that TiB_2 is chemically stable in both matrices up to 1573 K, however, TiB_2 was found to be less active in NiAl than in Ni_3Al due to lower nickel activity in NiAl.

1. Introduction

The interest in extending gas turbine engine operating temperatures to levels unattainable with conventional nickel-based superalloys has prompted searches for more advanced materials. Monolithic nickel aluminides (i.e. Ni_3Al and NiAl) are promising candidates due to their oxidation resistance and higher melting temperatures and lower densities than superalloys. Unfortunately, low ambient tensile ductility and insufficient high-temperature strength and creep resistance limit their application as single-phase materials [1]. Microalloying additions of boron have increased the ambient tensile ductility of Ni_3Al [2, 3] while alloying [4] and grain-size refinement [5, 6] have produced limited improvements in NiAl. Measurement of low tensile ductility has lead researchers to believe that these materials have low fracture toughness; however, recent work [7] has shown that this is not necessarily true.

Composite ceramic reinforcement approaches have been investigated to improve the above insufficient properties without altering the desirable properties of the monolithics. The addition of lower density ceramic materials (i.e. oxides, carbides, nitrides, etc.) will also decrease the composite density and hopefully lead to increased specific properties [8]. In the past five years, considerable research has focused on developing intermetallic matrix composites and has emphasized [8, 9] processing developments, interfacial compatibility optimization and mechanical property characterization.

The first section of this report reviews the chemical stability of candidate ceramic reinforcements in Ni_3Al and NiAl matrices from previous thermodynamic and experimental analyses. In the remaining sections, the chemical stability of one reinforcement material, titanium diboride (TiB_2), in Ni_3Al, Ni_3Al + B and NiAl matrices is investigated in depth. Thermodynamic calculations, X-ray diffraction analyses, Auger electron spectroscopy and transmission electron microscopy are among the experimental methods used to ascertain their stability and is a continuation of work presented earlier [10]. The ambient toughness [11] and strength [12] of the composites discussed here are presented elsewhere.

1.1. Review of stability of other reinforcements

Several boron-doped Ni_3Al alloys have been developed to improve the mechanical properties of Ni_3Al (γ'). Alloying element additions include the following: ambient tensile ductility enhancement with boron; high-temperature strength improvement with zirconium and/or hafnium; dynamic embrittlement elimination with chromium; and fabricability improvements with iron additions. Many alloys have incorporated these elements to various levels and been identified with designations, including the following [8, 13]: IC-15 (Ni–24.0 at % Al–0.24 at % B), IC-50 (Ni–23 at % Al–0.5 at % Hf–0.2 at % B), IC-218 (Ni–16.5 at % Al–8.0 at % Cr–0.4 at % Zr–0.1 at % B), IC-221 (Ni–16 at % Al–8.0 at % Cr–1 at % Zr–0.1 at % B) and IC-396M (Ni–16 at % Al–8 at % Cr–1.7 at % Mo–0.5 at % Zr–0.02 at % B). Composites of these matrices have been produced most exclusively by conventional powder consolidation processes, i.e. vacuum hot-pressing (VHP) and hot isostatic pressing (HIP). Reaction processing techniques [9, 14–17] have also been utilized; reaction sintering (RS), reaction hot-pressing (RHP) and reaction hot isostatic pressing (RHIP). Tables I–III review and summarize the results of stability analyses for

0022–2461

TABLE I Observations of ceramic reinforcement stability in Ni_3Al matrix composites

Reinforcement material	Matrix	Processing techniques and observations of interaction
Al_2O_3 (FP Type I)	IC-15	VHP at 1623 K for 1 h. Good bonding, no extensive interaction [18]
	IC-218	VHP at 1473 K for 1.5 h. No extensive interaction [18] SEM and TEM analysis showed 1–2 μm ZrO_2 particles at Al_2O_3/matrix interface due to Zr in alloy reacting with oxygen in powders, not with reinforcement; poor mechanical behavior results
	RHIP Ni_3Al + B	No interaction after RHIP (1073 K, 0.5 h) of IC-15 matrix [9, 14–17]
Al_2O_3 (Saphikon)	IC-221	VHP at 1173 K for 1 h, anneal at 1273 K up to 50 h. Little reaction noted, although Zr precipitates observed on matrix side of interface [19, 20]
Y_2O_3	RHIP Ni_3Al + B	No reaction following RHIP of IC-15 at 1073 K for 0.5 h [14, 15]
HfO_2	IC-396M	Hot extrusion at 1413 K, exposure at 1373 K for 24 h and 1073 for 24 h; no reaction noted [13]
ThO_2	IC-50	Mechanically alloyed, HIP at 1573 K for 3 h no reaction observed [21]
B_4C	IC-221	Unsuitable reinforcement, reactions observed. Nickel borides formed at the interfaces before dissolution; Ni diffused into the fibres [21]
B_4C/B	IC-221	Extensive reaction at as low as 1053 K during VHP. Nickel borides formed at the interfaces; Ni diffused into the fibres [8]
Al_2O_3 on B_4C/B	IC-221	CVD 1 μm Al_2O_3 on fibre, VHP at 1173 for 1 h, -no reaction; 1573 K, 3–6 h anneal minimal reaction; 1673 K anneal extensive reaction [8, 20]
SiC (SCS-6)	IC-50	Diffusion bonded 1373 K, 1 h; multi(4)layer reaction product; Hf and B not present in reaction layers, Ni diffusion to SiC, and no Si or C found in aluminide. Ni dominant diffusion species. Reaction rate 5 times slower than in superalloy/SiC [8, 23]
	IC-218	VHP at 1053–1253 K, 1 h at pressure; multi-layered reaction product on matrix side increasing in extent with temperature [22, 24]
	IC-221	1263 and 1373 K for 1 h, reactions observed [25]
	RHIP Ni_3Al + B (IC-15)	Severe during reaction processing at 1073 K for 10 min; High reaction temperature reached due to exotherm [15, 22, 24]
SiC	IC-50	Severe reaction noted after reaction bonding at 1173 K for 1 h. A four-layer reaction product produced [8]
SiC (Sigma)	IC-218	Rapid reaction at 1173 K for 1 h; 4 h complete reaction. Multi-layered reaction product [26]
	Ni_3Al (24 at % Al)	Reaction at 1273 K produced a reaction product consisting of $Ni_{5.4}AlSi_2$, NiAl and C precipitates [27, 28]
Y_2O_3 on SCS-6	RHIP Ni_3Al + B (IC-15)	No reaction took place during RHIP [22] consistent with other findings [29]
HfC on SCS-6	IC-221	Reaction below C-rich layer on fibre at 1173 K. [19] Not suitable as reaction barrier coating as suggested by tests with superalloys [29]
TaC on SCS-6	IC-221	Reaction below C-rich layer on fibre at 1173 K. [19] Not suitable as reaction barrier coating as suggested by tests with superalloys [19, 30]
Al_2O_3 on SCS-6	IC-221	Diffusion barrier coating suppressed reactions with matrix [8]
TiC	IC-221	Slight reaction after VHP and annealing at 1373 K for 100 h; 10–20 μm reaction zone on matrix side of reinforcement. EDAX analysis indicated Ti diffusion out of TiC, Zr into TiC and Cr accumulation at interface. No Al or Ni diffuse into reinforcement, C precipitates in TiC [19]
	IC-221	Consolidation then exposure at 1373 K for 1000 h; good bonding. Higher Zr and B levels detected (EDAX) at TiC surface [31, 32]
NbC	IC-396M	Hot extrusion at 1413 K, exposure at 1373 K for 24 h and 1073 K for 24 h; no reaction noted [13]
HfN	IC-396M	Hot extrusion at 1413 K, exposure at 1373 K for 24 h and 1073 K for 24 h; reaction observed [13]
TiN	IC-396M	Hot extrusion at 1413 K, exposure at 1373 K for 24 h and 1073 K for 24 h; no reaction noted [13]

several reinforcement materials in these Ni_3Al alloys as well as NiAl matrices.

Table I lists over 25 Ni_3Al matrix composites that have been produced. The reinforcement materials can be classified into three groups, including oxides (Al_2O_3 [9, 14–20], Y_2O_3 [14, 15], HfO_2 [13] and ThO_2 [21]), carbides (B_4C [8, 22], SiC [8, 15, 21–30], TiC [19, 31–32] and NbC [13]), and nitrides (HfN [13] and TiN [13]). In general, the oxides remained unreactive. However, in a few Al_2O_3 reinforced materials the interfacial bonds were weak, resulting in poor mechanical properties. Silicon carbide (SiC) fibres (SCS-6 and Sigma) reacted significantly with all alloy types. The compositions and reaction kinetics for formation of the reaction zones (comprised of four to six distinct layers) have been analysed for several cases and it was concluded that nickel was the dominant diffusing species. Application of oxide (Al_2O_3 and Y_2O_3) diffusion barrier coatings prevented or reduced reaction by inhibiting nickel diffusion. Boron carbide (B_4C) fibres also reacted severely with the Ni_3Al matrices, but application of an Al_2O_3 coating again prevented reaction. Titanium carbide (TiC) and NbC appear to be stable in the Ni_3Al materials.

TABLE II Compatibility of ceramic reinforcements in NiAl matrices

Reinforcement name and shape	Ceramic composition	Observations
Nextel 480 fibres	10 wt % Al_2O_3, 28 wt % SiO_2, 2 wt % B_2O_3	Reactions observed after powder cloth processing and VHP at 1573 K for 3 to 6 h [33]
Sumitomo fibres	85 wt % Al_2O_3 15 wt % SiO_2	Reactions observed after powder cloth processing and VHP at 1573 K for 3–6 h [33]
Tyranno fibres	Si–C-Ti–O	Reactions during powder cloth processing and VHP at 1573 K for 3–6 h [33]
American matrix whiskers	α-SiC	Stable in matrix [33]
Sigma SiC fibres	β-SiC	Reaction observed after powder cloth processing, VHP, and annealing at 1473 K, 50 h [34]
SiC plates	β-SiC	1373 K and 1473 K no reaction. 1573 K reaction–diffusion of Si and C into NiAl produced $Ni_{14}Al_9Si_2$ containing C precipitates [35]
SiC particulates	β-SiC	1580 K, 3 h at pressure during hot-pressing no reaction recorded [36]
SiC particulates	β-SiC	Extensive reaction after XD processing and VHP at 1173 K for 4 h [37]
Tokai whiskers	Si_3N_4	Reaction with the matrix [33]
Si_3N_4 wafer	Si_3N_4	1613 K, 3 h stable but surface reaction observed [36]
Norton ZrO_2 particulates[a]	ZrO_2, CaO	Reactions after powder cloth processing and VHP at 1573 K for 3–6 h [33]
Y_2O_3 particulates[a]	Y_2O_3	Reactions after powder cloth processing and VHP at 1573 K for 3–6 h [33]
Y_2O_3 particulates	Y_2O_3	Preliminary results indicate stability during 1613 K heat treatment [36]
AlN particulates[a]	AlN	VHP at 1573 K for 3–6 h. Stable in matrix [33]
Al_2O_3 fibers	Al_2O_3	No reaction observed [36, 38]
Saphikon fibres	Al_2O_3	VHP at 1813 K, for 3 h; no reaction [36]
FP fibres	Al_2O_3	VHP at 1813 K for 3 h; no reaction [36]
TiC particles	TiC	VHP at 1813 K for 3 h; stable [36]
W wire/fibres	W	No reaction observed [38]
B_4C particulates	B_4C	Extensive reaction after XD processing and VHP at 1173 K for 4 h. Dissolved in matrix [37]
$TiBe_{12}$	$TiBe_{12}$	Reaction product is $NiAlBe_2$; after 1300 K for 100 h 20–25 μm reaction zone as fabricated, 95 μm after anneal [39]
Nb_2Be_{17} plates	Nb_2Be_{17}	Extensive reaction after VHP at 1373 K for 2 h. Three distinct 30–40 to 50–60 μm thick layers in NiAl detected by EDS analysis [40]
Oxidized Nb_2Be_{17} plates	BeO diffusion barrier coating on Nb_2Be_{17}	VHP diffusion bonded at 373 for 2 h. Good bonding, no reaction in as processed condition or after 100 h. At 1473 K for 100 h, reaction took place [40]

[a] Theoretically, (Table III), these materials are stable in NiAl. Reactions may have taken place with binder materials rather than NiAl during processing.

TABLE III Compatible reinforcement materials in NiAl to 1573 K as determined by thermodynamic analysis [41]

Carbides	Borides	Oxides	Nitrides	Silicides
HfC	HfB_2	Al_2O_3, La_2O_3	AlN	Mo_3Si
TiC	ScB_2	BeO, Sc_2O_3	HfN	Mo_5Si_3
ZrC	TiB_2	CaO, Y_2O_3	TiN	
NbC	CrB_2	Gd_2O_3, ZrO_2	ZrN	
TaC		HfO_2, $CaZrO_3$		
Ta_2C		Ca_2O_3, $Y_2O_3 \cdot 2ZrO_2$		

Table II presents experimental results of compatibility between NiAl (mainly the stoichiometric composition) and various ceramic reinforcements [33-41]. Alumina (Al_2O_3) [36, 38], Y_2O_3 (as reported by Shah *et al.* [36]), AlN [33], TiC [36] and non-reactive tungsten [38] are stable in NiAl alloys at elevated temperatures, whereas Nextel 480 fibres [33], Sumitomo fibres [33], Tyranno fibres [33], SiC fibres [34] and plates [35] and particulates [36, 37], Tokai whiskers (Si_3N_4) [33], Norton ZrO_2 particulates [33], Y_2O_3 particulates [33], B_4C particulates, $TiBe_{12}$ [39] and Nb_2Be_{17} [40] are all unstable. As indicated in the table, three systems which showed instability [36] may have reacted with binder materials used in powder cloth processing rather than with NiAl matrices. As will be shown, thermodynamic calculations predicted stability for these materials systems.

A thermodynamic analysis developed by Misra [41] has identified stable ceramic reinforcement materials for NiAl composites. Table III lists the potentially stable oxides, carbides, nitrides, borides and silicides from about 80 materials analysed. In the analysis it was noted that the level of compatibility was significantly affected by reaction temperature and matrix stoichiometry. It is useful to realise that these calculations are a useful first approximation of potential behaviour but, experimental verification is necessary to assess actual response and to investigate the compatibility of other properties (i.e. thermal).

1.2. Composites in this study

Selection of reinforcement for a composite system requires mechanical/thermal compatibility and the chemical stability within the matrix [8]. In high-temperature applications in which high specific stiffnesses and strengths are needed, materials with high elastic moduli and strengths, and low specific gravities, are desirable. Thermal expansion mismatch should be minimized to reduce the possibility of cracking that could result from residual streses generated during processing or application. In many of these composite materials, interfacial bond strength is desir-

able; however, overgrowth of reaction layers (chemical instability) would be detrimental [8].

Titanium diboride (TiB_2) was selected as a candidate reinforcement material for stability analysis. The attractive physical and mechanical properties include low specific gravity (4.52 $g\,cm^{-3}$) and high room-temperature elastic modulus (414 GPa), and compressive strength (670 MPa) which do not decrease substantially even at higher temperatures [42–45]. Flexural strength of TiB_2 is 241 MPa at 298 K, increasing to 303 MPa at 1773 K, then decreasing monotonically to 241 MPa at 2273 K [46]. No plastic deformation has been observed in this ceramic to temperatures as high as 1973 K [47]. The hardness of TiB_2 ($\approx$3400 VHN at room temperature decreasing to 220 at 1973 K) is higher than that of Ni_3Al (VHN 100–255) and NiAl (VHN 240–435). Unfortunately, a thermal expansion coefficient mismatch of $\approx 7 \times 10^{-6}\,K^{-1}$ exists between TiB_2 and Ni_3Al and NiAl over a wide temperature range (Fig. 1) [48]. In spite of exhibiting poor high-temperature oxidation characteristics [45–51], incorporating TiB_2 in an oxidation-resistant nickel aluminide matrix may shield it from detrimental atmospheres.

2. Experimental procedure

Materials in this study were vacuum (1×10^{-4} torr; 1 torr = 133.322 Pa) hot-pressed from blends of prealloyed matrix powders and particulate reinforcement. The spherical matrix powders (Alloy Metals Inc.) had nominal compositions of Ni_3Al (24 at % Al) and NiAl (45 at % Al) and were gas-atomized from prealloyed melts (Fig. 2). Boron-doped Ni_3Al (24 at % Al, 0.2 at % B) was prepared for processing by blending -200 mesh elemental boron powder with prealloyed Ni_3Al. Composite powders were made by vee-blending 10 vol % TiB_2 reinforcement particles with prealloyed matrix powders. The chemical vapour deposited TiB_2 particles (Union Carbide Corporation) were hexagonal platelets with an aspect ratio of 4:1 (Fig. 3). The composition of the powder as given by the supplier was Ti–33.14 at % B, 0.38 at % C, 1.22 at % O, 0.08 at % N and 0.01 at % Fe. The monolithic and composite structures were consolidated at 1373 K (Ni_3Al) or 1623 K (NiAl) at 48 MPa for 2–4 h.

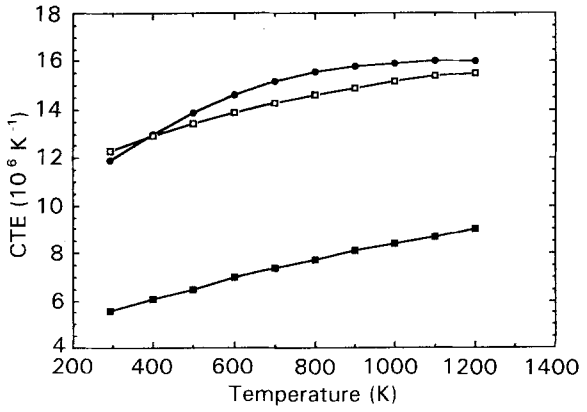

Figure 1 Thermal expansion coefficients for (■) TiB_2, (●) NiAl and (□) Ni_3Al as a function of temperature [48].

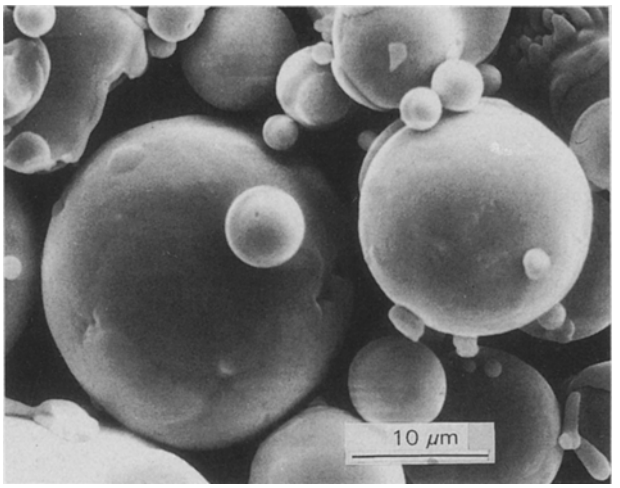

Figure 2 Scanning electron micrograph of fine gas-atomized Ni_3Al powder showing spherical morphology.

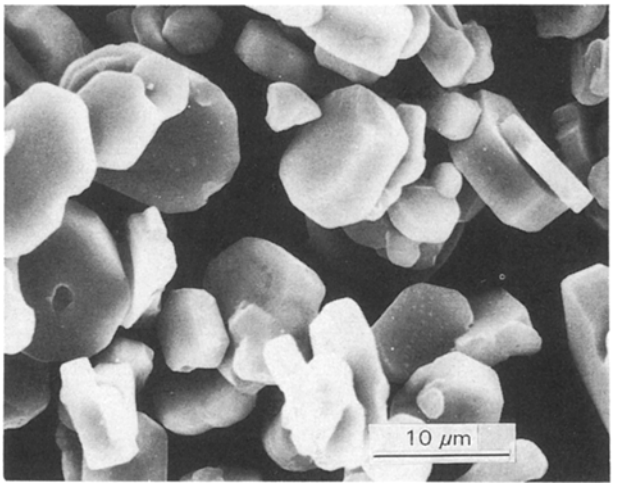

Figure 3 Scanning electron micrograph of coarse TiB_2 particles showing hexagonal-disc morphology with diameter to height ratio of 4:1

Polished as-hot-pressed composite microstructures were examined using a Jeol 840A scanning electron microscope at an accelerating voltage of 25 kV for imaging or 15 kV for semiquantitative energy dispersive X-ray analysis (EDAX). The EDAX capabilities (Tracor Northern) were utilized to monitor the extent of diffusing species near TiB_2 particle/matrix interfaces (to within 5 μm from the particles in the aluminide), within the matrix about 50 μm from any particles and within TiB_2 particles. A number of scans (10–15) for nickel, aluminium and titanium were made at each location and average values computed for comparison between sites and composite types. Diffusion profiles across interfaces were quantified using Auger electron spectroscopy analyses (Phi 660 scanning Auger microscope) with a beam resolution of 80 nm, accelerating voltage of 10 kV and target current of 20 nA. A 10 nm surface layer was removed by argon sputtering prior to the line scans for nickel, aluminium, boron, titanium, carbon and oxygen across matrix/particle interfaces.

In addition to the other electron microscopy techniques, conventional transmission electron microscopy was employed to image matrix/particle interfacial regions in thin foils prepared from the hot-pressed discs. Samples were initially thinned and polished to $\approx 150\,\mu m$, punched to 3 mm discs and prepared by standard jet polishing techniques using a 5 vol % perchloric acid and 95 vol % methanol bath held at 233 K and current maintained at 15 V. A Phillips EM400T operating at an accelerating voltage of 120 kV was used for the imaging.

X-ray diffraction (XRD) techniques were used to identify product phases (if any) and determine lattice parameters (or expansion due to diffusion) in the nickel aluminide powders, monolithics and composite matrices. The room-temperature XRD (monochromatic CuK_α radiation, $\lambda = 0.154\,18$ nm) was performed on a Phillips autodiffractometer interfaced with an IBM PC for data collection. Step scans for phase identification were made from $2\theta = 20°$–$125°$, a step of 0.05° and a hold time of 10 s at each step. Lattice parameters were determined after scanning at higher 2θ positions, stepping 0.01° and holding for 2 s at each position. *Specplot* software on a VAX PDP-11 system helped determine precise positions and relative intensities of peaks. Cohen's least-squares method [52] was used in calculating lattice parameters.

Equilibrium thermodynamic calculations were made to investigate reaction at 1173, 1373 and 1573 K between Ni_3Al (over the range of stoichiometry) and TiB_2, as was previously completed for the NiAl–TiB_2 system. Hot-pressing for the experiments was conducted over this temperature range. The possibility of forming a reaction product or dissolving the reinforcement in the matrices was investigated. The general details of the analysis are presented elsewhere [41, 53], but the specific details for the current systems are discussed in the following section. The results of the calculations are later compared to those obtained by analytical techniques.

3. Results and discussion

3.1. Thermodynamic analysis

3.1.1. Thermodynamics of the system and the analysis

The thermodynamic calculations, based on an already established model [41, 53], consider three categories of reactions between matrix and reinforcement. The first assumes single-element interactions (one element from each the binary matrix and binary reinforcement) producing only one binary compound. The second considers formation of two binary compounds by reactions of one or both matrix elements with the reinforcement material. If these reactions are not possible, dissolution of the reinforcement elements in the matrix is the last considered. The purpose of this analysis was to determine if reaction products are created or if extensive dissolution is possible, both of which indicate an unstable composite system. The first step of the process is identification of possible stable reaction products from appropriate binary phase diagrams. Only binary products are considered due to the unavailability of thermodynamic data for ternary and higher order compounds and is sufficient for first-order approximation. In the present systems, possible products can be identified from the Ni–Ti, Ni–B, Al–Ti, and Al–B phase diagrams at the reaction temperatures investigated (1173, 1373 and 1573 K). Sufficient quantity of reactants are assumed to be present allowing production of any phase across each diagram.

Further analysis requires use of thermodynamic quantities, including the activities of nickel and aluminium in Ni_3Al and NiAl with changes in stoichiometry, in addition to the standard free energies of formation of the reinforcement (TiB_2) and possible binary reaction products. In the Ni–Al phase diagram [54], NiAl exists over a wide range of stoichiometry from 31–58 at % Al while Ni_3Al exists over a narrower range of 24–27 at % Al. The aluminium activities, a_{Al} in the Ni–Al system over the composition range have been measured at 1273 K by Steiner and Komarek [55]; nickel activities, a_{Ni}, at the same temperature were subsequently calculated by Hanneman and Seybolt [56]. In NiAl, a_{Al} increases sharply between 48 and 52 at % Al, the steepest rise occurring at 50 at % Al [41]. The a_{Al} values in Ni_3Al are much lower (a_{Ni} much higher) than those in NiAl and do not vary drastically with composition. In order to perform calculations for several temperatures (1173, 1373 and 1573 K), the a_{Al} and a_{Ni} (a_X) values had to be interpolated from the 1273 K data [41] using the following equation

$$(T_2)\log a_{X(\text{at}\,T_2)} - (T_1)\log a_{X(\text{at}\,T_1)} = \frac{\Delta\bar{H}_X}{19.14}\left(\frac{1}{T_2} - \frac{1}{T_1}\right)$$

where $\Delta\bar{H}_{Al}$ and $\Delta\bar{H}_{Ni}$ ($\Delta\bar{H}_X$) are the partial molar enthalpies of aluminium and nickel, respectively, and T_1 and T_2 are two different temperatures. The $\Delta\bar{H}_{Al}$ and $\Delta\bar{H}_{Ni}$ values for Ni_3Al are $-133\,890$ and $-12\,550$ kJ g·atom^{-1}, respectively as determined from Misra [41], Steiner and Komarek [55], and Bernie *et al.* [57]. For sub-stoichiometric NiAl (at % Al < 50) $\Delta\bar{H}_{Al}$ and $\Delta\bar{H}_{Ni}$ are $-121\,340$ and $-16\,740$ kJ g·atom^{-1}, respectively, while above 50 at % Al, these values change significantly to $-29\,290$ and $-104\,600$ kJ g·mol^{-1}; the drastic change is observed at stoichiometric composition. The a_{Al} and a_{Ni} values calculated based on Misra's (NiAl) and the present calculations (Ni_3Al) are listed in Tables IV and V, respectively.

The standard free energies of formation; (ΔG_f°), for the potential product compounds from the Ni–Ti, Ni–B, Al–Ti, and Al–B phase diagrams at the three temperatures are listed in Table VI. Most of the data collected was reported from other references by Misra [41]; however, values for Ti_2Ni [58] and $TiAl_3$ [59] were estimated from phase-diagram predictions. The ΔG_f° values at 1173 K were estimated from those at the higher temperatures through manipulations of the Gibbs–Helmholtz equation.

Given the thermodynamic information, the stability analysis could be undertaken. The following calculations were made assuming equilibrium is reached

TABLE IV Activity of aluminium and nickel in NiAl (β phase) at various temperatures and compositions [41]

Temp. (K)	Al(at%)	a_{Al}	a_{Ni}
1373	38	1.06×10^{-4}	0.419
	40	1.38×10^{-4}	0.355
	42	1.84×10^{-4}	0.294
	44	2.42×10^{-4}	0.238
	46	3.76×10^{-4}	0.167
	48	7.84×10^{-4}	0.087
	49	1.33×10^{-3}	0.051
	49.5	2.35×10^{-3}	0.036
	50	4.16×10^{-3}	0.016
	50.5	9.97×10^{-3}	6.21×10^{-3}
	51	0.016	4.41×10^{-3}
	52	0.026	2.54×10^{-3}
	54	0.026	1.23×10^{-3}
1573	38	4.11×10^{-4}	0.476
	40	5.36×10^{-4}	0.403
	42	7.15×10^{-4}	0.333
	44	9.38×10^{-4}	0.271
	46	1.45×10^{-3}	0.190
	48	3.04×10^{-3}	0.099
	49	5.15×10^{-3}	0.058
	49.5	9.11×10^{-3}	0.042
	50	9.81×10^{-3}	0.030
	50.5	0.014	8.53×10^{-3}
	51	0.022	3.49×10^{-3}
	52	0.037	2.70×10^{-3}
	54	0.071	1.71×10^{-3}

TABLE V Activity of aluminium and nickel in Ni_3Al (γ' phase) at various temperatures at the phase boundaries as calculated in this study

Temp. (K)	Al (at %)	a_{Al}	a_{Ni}
1173	24	1.07×10^{-5}	0.685
	27	2.64×10^{-5}	0.482
1373	24	5.67×10^{-5}	0.709
	27	1.23×10^{-4}	0.535
1573	24	1.97×10^{-4}	0.741
	27	3.86×10^{-4}	0.580

which requires a_{Al} and/or a_{Ni} values to remain numerically the same in all locations in the system, i.e. keep values in Tables IV and V. The essential steps are outlined below and can be repeated for each matrix, matrix composition and temperature.

(a) *Identify potential product compounds from the appropriate binary phase diagrams (Ni–B, Ni–Ti, Al–B and Al–Ti)*. Selection is made by establishing reaction equations between the elements and the binary compounds, using equilibrium constants (K, determined from ΔG_f°), assuming a value of 1 for a_{Ti} or a_B and calculating a_{Al} or a_{Ni}. The known tabulated values must exceed the calculated activities lower for the reaction to proceed and the product to be potentially stable. Several compounds may be found from each binary system.

(b) *Determine the most stable compound from each phase diagram.* Using the same equilibrium equations established in (a), a_{Ti} or a_B values for each compound selected from a phase diagram can be calculated using

TABLE VI Standard free energies of formation (kJ/mole) for the potential binary reaction products [41].

Compound	Standard free energy of formation (kJ mol^{-1})		
	1173 K	1373 K	1573 K
AlB_{12}	− 212.1	− 211.3	− 210.0
Ni_2B	− 54.0	− 66.5	− 79.1
Ni_3B	− 67.4	− 78.2	[a]
Ti_2Ni[b]	− 24.4	[a]	[a]
TiNi	− 55.6	− 52.3	− 49.0
$TiNi_3$	− 115.5	− 109.2	− 102.09
Ti_3Al	− 68.2	− 61.5	− 54.8
TiAl	− 59.2	− 59.8	− 60.7
$TiAl_3$[b]	− 25.2	− 22.9	− 20.6
TiB_2	− 260.2	− 255.6	− 251.0

[a] These phases do not exist at these temperatures.
[b] Thermodynamic estimated data from references [58, 59].

K-values and tabulated a_{Al} or a_{Ni} values. Only one compound will form with the least possible a_{Ti} or a_B value. This is considered the most stable compound from that phase diagram; however, this does not necessarily mean that this will form, as will be seen in steps (c)–(e). One compound from each phase diagram can be identified.

(c) *Select the most stable Ti- or B-containing compound.* Under equilibrium conditions, reactions of titanium and boron with nickel or aluminium will produce only one compound. The relative stability of the two titanium or boron compounds from (b) can be determined by setting up equilibrium equations between them. Using equilibrium constants and known a_{Al} and a_{Ni} values, one can determine which of the two will have the greater tendency to form. Two compounds (one boron- and the other titanium-containing) can be determined from the four phase diagrams.

(d) *Determine if one product compound can form.* Setting up an equilibrium equation between TiB_2 and the appropriate matrix element (nickel or aluminium) to form one of the two potentially stable compounds from (c), we can find if the reaction will take place. If the free energy of the reaction is negative *and* calculated a_{Al} or a_{Ni} values needed to produce the reaction (from the appropriate K-value) are less than the equilibrium values (Tables IV and V) then a reaction product will form and the matrix/TiB_2 system is unstable. If not, production of both compounds from (c) together is considered.

(e) *Determine if dual-product compounds form simultaneously.* The equilibrium equation between TiB_2 with matrix element(s) and both potentially stable compounds from (c) can be set up to find if this reaction will take place. If ΔG_f° of this reaction is negative *and* calculated a_{Al} or a_{Ni} values required to produce the reaction (from the appropriate K-value) are less than the equilibrium matrix values (Table IV and V) then both reaction products will form and the matrix/TiB_2 system is considered unstable. If not, dissolution of titanium and boron in the matrix is next to be considered.

(f) *Determine the minimum activity of titanium and boron in the matrices after dissolution.* Using earlier equilibrium equations for single product formation (from (c)), the maximum activity of titanium or boron just before the product would form can be determined. Setting up an equilibrium equation between TiB_2 and titanium and boron, we can then calculate the minimum activity of one element (a_{Ti} or a_B) knowing the maximum of the other from the previous calculation. This treatment assumes that only titanium and boron diffuse into the matrix alloy but nickel or aluminium do not diffuse into the TiB_2 or if they did, the mechanical properties would remain unaffected. The minimum extent of dissolution in terms of mole fraction, X_i, of titanium or boron in the matrix could be inferred by this activity value, through the activity coefficient, γ_1 or $a_i = \gamma_i X_1$. This coefficient, ranging from 0–1, is unknown in these systems; however, Misra adopted a cut-off activity value, a_i, of 10^{-3}, if exceeded, dissolution is regarded as too extensive for the system to be considered stable.

3.1.2. Results for NiAl- and Ni_3Al–TiB_2 systems

The calculations in the previous section were conducted by Misra [41] for the NiAl/TiB_2 system as a function of temperature and NiAl stoichiometry, and similarly in this report for the Ni_3Al/TiB_2 system. The results are presented in Tables VII and VIII. A number of potentially stable compounds were identified from the four binary phase diagrams. For the Ni_3Al/TiB_2 composite system the most stable binary compounds were found to be AlB_{12}, Ni_2B, Ni_3Ti and Ti_3Al. Selection of the titanium- and boron-containing compound provided those found in Table VII, indicating a strong effect of matrix composition, stoichiometry and temperature on the possible reaction products, especially in the NiAl system due to drastic changes in elemental activities with stoichiometry. The results show that Ni_3Al/TiB_2 is less affected by changes in temperature and compositional variations.

Further calculations indicated that single and dual reaction products would not form over the range of compositions and temperatures tested, although the free energies of reaction were negative for all the cases investigated. Treatment of titanium and boron dissolution in the matrices yielded the results in Table VIII; calculations for 44 and 46 at % NiAl (alloy investigated experimentally in this study had a nominal composition of 45 at % Al) and 24 and 27 at % Al, Ni_3Al are included. Minimum activities of titanium and boron in either matrix are shown to increase as the nickel content (and activity) increases or as reaction temperatures rise. The a_B (min) are an order of magnitude and a_{Ti} (min) several orders of magnitude less in NiAl than in Ni_3Al.

Comparison of the activity values suggests that TiB_2 is more stable in NiAl (44 and 46 at % Al) than in Ni_3Al matrices. The titanium and boron activities are generally less than the cut-off (10^{-3}) value defined by Misra for stability for all the materials. Boron is observed to have a relatively high activity in Ni_3Al (Table VIII); however, it is known that the boron is insoluble and increases room-temperature ductility of Ni_3Al [1, 2]. The minimum activity of titanium approaches higher values at 1573 K in Ni_3Al, especially in the higher nickel-containing Ni_3Al, but remains low in NiAl. Although titanium activity in the matrices has been calculated it is unknown what levels can be obtained, as the activity coefficient is not known ($a_i = \gamma_i X_i$). Solubility estimations of titanium in NiAl and in Ni_3Al (Table IX) were made using isothermal sections in the Ni–Al–Ti phase diagram [60] and indicate that high values *are* possible in both phases at the temperatures of interest. Values of 16–17 at % Ti in Ni_3Al and 7–10 at % Ti in NiAl are possible between 1073 and 1423 K, respectively. Although these values are high, this does not necessarily indicate that these levels can be reached in these composite systems without considering equilibrium thermodyn-

TABLE VII Potentially stable reaction products from interaction of titanium or boron with NiAl or Ni_3Al.

Matrix–element	Temp. (K)	Al (at %)	Potentially stable compound
NiAl–B	1373 and 1573	< 49	AlB_{12}[a]
		> 49	Ni_2B[a]
		> 50.3	AlTi[a]
NiAl–Ti	1373	49–50	NiTi[a]
		< 49	Ni_3Ti[a]
Ni_3Al–B	1173–1573	24–27	Ni_2B[b]
Ni_3Al–Ti	1173–1573	24–27	Ni_3Ti[b]

[a] Determined by Misra [41].
[b] Determined in this study.

TABLE VIII Minimum calculated activities for titanium and boron in Ni_3Al and NiAl after dissolution of TiB_2.

Temp. (K)	Minimum activity	Ni_3Al: 24 at % Al[a]	Ni_3Al: 27 at % Al[a]	NiAl: 44 at % Al[b]	NiAl: 46 at % Al[b]
1173	a_B(min)	3.4×10^{-4}	2.0×10^{-4}	[c]	[c]
	a_{Ti}(min)	3.63×10^{-8}	8.9×10^{-9}	[c]	[c]
1373	a_B(min)	3.09×10^{-3}	2.03×10^{-3}	1.89×10^{-4}	1.10×10^{-4}
	a_{Ti}(min)	5.48×10^{-6}	1.80×10^{-6}	1.17×10^{-7}	1.68×10^{-8}
1573	a_B(min)	2.20×10^{-3}	1.54×10^{-3}	4.87×10^{-4}	2.86×10^{-4}
	a_{Ti}(min)	2.50×10^{-4}	9.30×10^{-5}	6.52×10^{-7}	1.57×10^{-7}

[a] As determined in this study.
[b] As determined by Misra [41].
[c] Analysis was not carried out at this temperature;

TABLE IX Solubilities of titanium in Ni_3Al and NiAl at 1073, 1300 and 1423 K as determined from the Ni–Al–Ti ternary phase diagram [60]

Temperature (K)	Ti solubility (at %)	
	Ni_3Al	NiAl
1073	16.1	6.9
1300	16.5	9.2
1423	17.1	10.2

amics (i.e. breakdown of TiB_2 into titanium and boron, etc.). Without actually measuring these titanium contents. Misra's cut-off minimum activity value (10^{-3}) can be used to evaluate those values in Table VIII; TiB_2, therefore, can be regarded as stable in Ni_3Al and much more stable in the NiAl (44 and 45 at % Al) to as high as 1573 K. The higher reactivity of TiB_2 ub Bu_3Al compared to TiB_2 in NiAl results from the higher nickel activity in Ni_3Al. Previous studies [27] have also shown SiC to be more reactive in Ni_3Al than in NiAl for this reason.

The results obtained by the thermodynamic calculations are consistent with the experimental findings presented in the following sections.

3.2. Electron microscopy analyses

Energy dispersive X-ray (EDAX) analysis using scanning electron microscopy (SEM), elemental surface analysis using Auger electron spectroscopy (AES), and interfacial imaging using conventional transmission electron microscopy (TEM) were all employed to investigate the possibility of chemical interaction between TiB_2 and the two matrix systems for comparison with the thermodynamic calculations. High-magnification SEM observation of interfacial areas in the Ni_3Al- and NiAl-based composites (Fig. 4) did not reveal the presence of distinct reaction products or zones, as predicted theoretically. Standardless semi-quantitative EDAX analysis was performed in three separate areas of each composite, at ~5 μm from TiB_2 particles in the matrix, in the centre of large matrix grains ~50 μm away from any reinforcement and within individual TiB_2 particles to attempt to quantify the diffusion of species. The average results of 10–15 scans were used to compare relative quantities of nickel, aluminum and titanium in three locations between each composite type. Analysis in the near-TiB_2 regions (~5 μm away) in the NiAl and Ni_3Al matrices indicated that the relative amounts of titanium were 0.91 and 5.24 at %, respectively, falling off to substantially lower values at the centre of the grains. The higher titanium contents in the regions in Ni_3Al neighbouring TiB_2, as compared to similar regions in NiAl, are consistent with the thermodynamic calculations which showed that titanium would have higher minimum activity in Ni_3Al than NiAl. Nickel was detected in TiB_2 particles to levels of ~2 at % in both composite types; no traces of aluminium were detected. These results suggest that titanium has diffused out of and nickel into TiB_2 during consolidation.

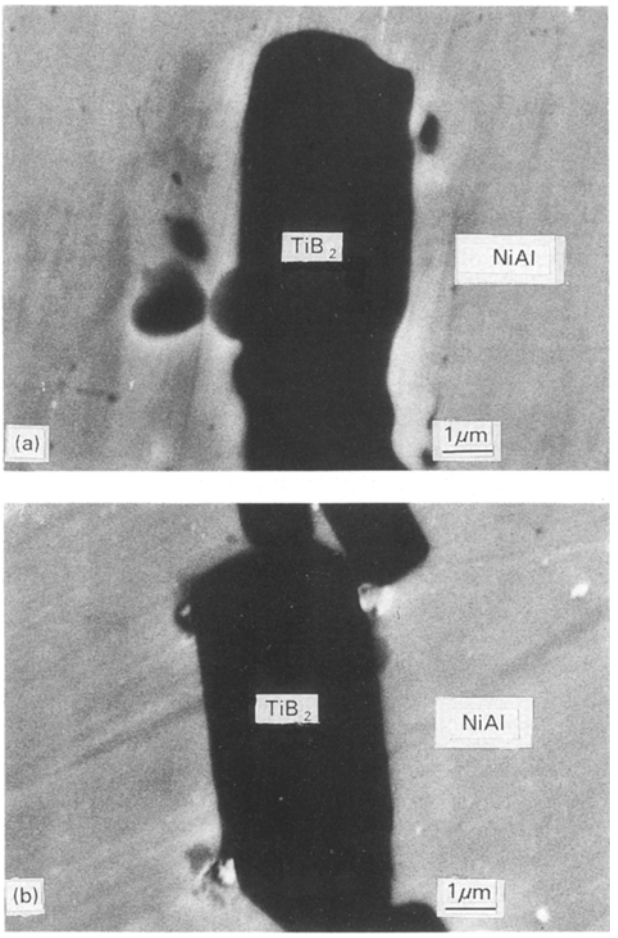

Figure 4 High-magnification scanning electron micrograph of TiB_2 reinforcement (a) Ni_3Al and (b) NiAl matrix interfacial regions showing no reaction product.

The presence and diffusion profiles of lighter elements not detectable by the presently used EDAX system as well as those detected before (nickel, aluminium and titanium) were quantified by AES surface analysis line scans across matrix/particle interfaces. Typical results showing the relative contents across the interfaces in Ni_3Al/TiB_2 and $NiAl/TiB_2$ at the same magnification are presented in Figs 5 and 6, respectively. A significant interdiffusion zone is apparent in the Ni_3Al/TiB_2 diffusion couple where titanium and boron have diffused into the matrix, while traces of nickel have diffused into the reinforcement. A similar scan in the NiAl composite indicates that extent of the interdiffusion is less in comparison than that found in the Ni_3Al-based materials. The results compare well with the EDAX results and again substantiate the thermodynamic calculations.

A typical transmission electron micrograph of TiB_2 particles in an NiAl matrix is pictured in Fig. 7. No continuous product phases or precipitates were observed in the interfaces to at least × 48 000 magnification. The composite interfaces were sharp and distinct indicative of a stable system. Dislocations were often observed in the matrix near particles, especially in locations between particles. This dislocation activity is believed to result from the CTE mismatch between the aluminides and TiB_2 (Fig. 1) resulting in dislocation punching during cool-down; as the dislocation densities in areas of the matrix away from the

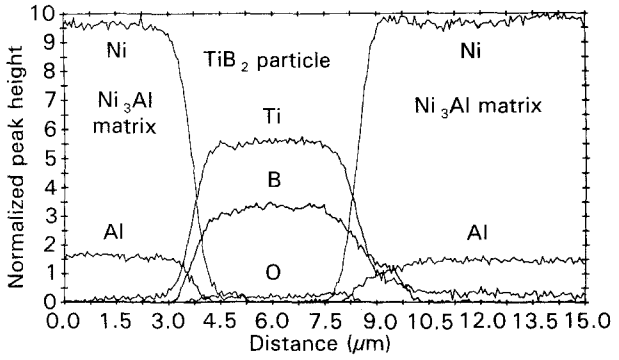

Figure 5 Scanning Auger electron line scans across an Ni_3Al/TiB_2 interface.

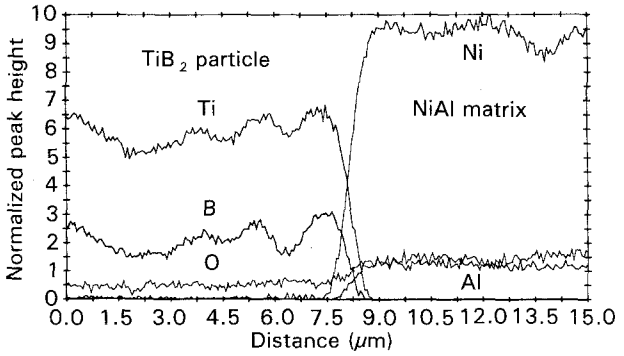

Figure 6 Scanning Auger electron line scans across an $NiAl/TiB_2$ interface.

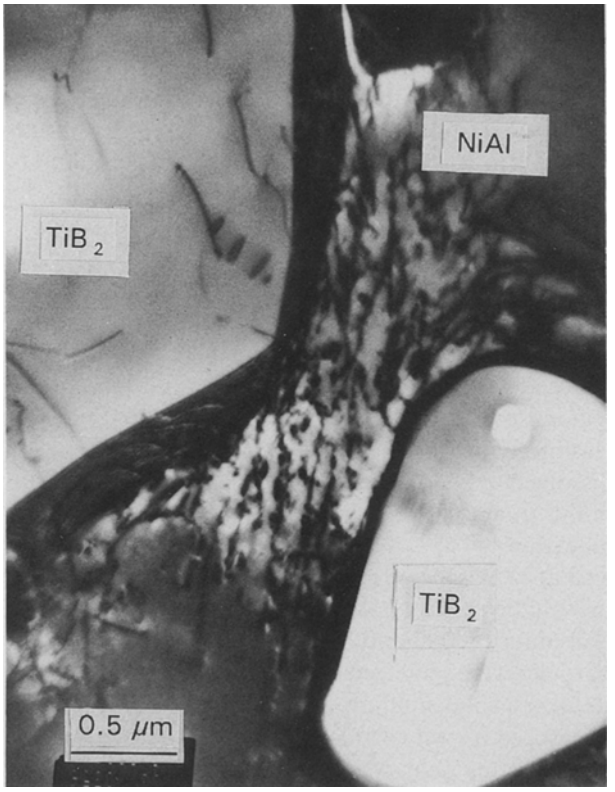

Figure 7 Typical interfacial region between TiB_2 particulates and NiAl matrix. No reaction products are observed in the interfaces.

reinforcement in the as-hot-pressed materials were significantly less. Conventional transmission electron micrographs from the Ni_3Al/TiB_2 interfacial regions at the same magnification also indicate a lack of reaction.

All these electron microscopy results on the hot-pressed microstructures are consistent with the thermodynamic calculations in the previous section. No reaction products were predicted to form, but slight dissolution is expected with higher activities and solubilities of titanium in Ni_3Al as compared to those values for titanium in NiAl under similar conditions. Although the NiAl composite was processed at a similar matrix homologous temperature (0.85 T_m) as the Ni_3Al-composite in this investigation, less titanium was present (as detected by EDAX and AES) in this as-hot-pressed matrix.

3.3. X-ray diffraction analyses

X-ray diffraction (XRD) techniques were also used to detect reaction products and measure lattice constants that may have changed with interdiffusion at matrix/reinforcement interfaces. Although in all cases, no reaction products were detected, some changes in lattice parameter were measured as a result of either oxygen pick-up during processing or slight dissolution reaction with TiB_2 (as suggested by the previous results). The lattice parameters of as-hot-pressed monolithic alloys, composite matrix alloys, and as-received powders are presented in Table X. For the NiAl-based materials, the lattice constants remained virtually unchanged throughout the processing conditions, with a constant of about 0.2883 nm for the 45 at % Al, NiAl. The absence of any interaction of NiAl-based materials with TiB_2 again supports the findings of the thermodynamic calculations and electron microscopy analyses.

The results from the Ni_3Al-based materials present different behaviour. Hot pressing of prealloyed powders into monolithic Ni_3Al produced some expansion of the lattice ($\approx$0.000 05 nm) from that measured in the powders, the change possibly resulting from oxygen pick-up and dissolution in the powder metallurgy (P/M) process. Boron additions (0.2–0.5 at %) to Ni_3Al powders produced significant increases in lattice parameter (Table X, $\approx$0.0003 nm) after densification, consistent with previous work [61, 62]. After blending and consolidating Ni_3Al (and + B) powders with TiB_2 particulates, considerable lattice dilation was also noted as compared to the monolithic materials. The increase in parameter of $\approx$0.0025 nm was partially attributed to the diffusion of titanium and boron into the matrices as detected previously by both AES and EDAX analyses in the matrix near Ni_3Al/TiB_2 interfaces. Titanium and boron can each increase the lattice spacings in Ni_3Al; however, previous results suggest that titanium has a greater effect owing to the relative sizes of the atoms and the solubilities obtainable in Ni_3Al.

Increases in lattice parameter with additions of titanium to Ni_3Al have been quantified by several authors. Ochiai *et al.* [63] used XRD methods to measure the broadening in lattice parameter with titanium addition to Ni_3Al in arc-melted and homogenized samples. A linear rate of increase in lattice

parameter, a, with concentration, c, of titanium was found: $da/dc = 2 \times 10^{-4}$ nm/at % Ti, as was also found by other investigators [64]. Guard and Westbrook [65] and others [66] also confirmed the expansion in lattice parameter, in addition to significant increases in hardness with small additions of titanium to Ni_3Al. The presently observed increases in the Ni_3Al-based composite matrices were of the order of ~ 0.0025 nm. Using the results determined by Ochiai *et al.*, 12.5 at % Ti is needed to cause this increase in lattice constant. Although this amount of titanium is within the solubility limits determined by the ternary phase diagram (Table IX) and may be possible in regions local to the TiB_2 particles, it is more than that feasible if the 10 vol % TiB_2 were homogeneously dissolved in Ni_3Al. Calculations show that dissolution of this quantity of titanium and boron yields a material with 69.47 at % Ni, 21.93 at % Al, 5.93 at % Ti and 2.68 at % B. One Ni_3Al-based composite produced in the studies [10], hot-pressed at temperatures well exceeding 1500 K and fully reacted (i.e. reinforcement particles were undetectable in optical microstructures) to form a solid solution with titanium and 2.5 at % B (measured by wet chemical analysis). The lattice parameter of this alloy was $0.357\,46 \pm 0.000\,01$ nm, a lattice parameter increase of 0.000 46 nm from that of pure Ni_3Al (24 at % Al). This increase is consistent with the ~ 6 at % Ti addition in the homogeneous case, as calculated using the results of Guard and Westbrook [65].

In composite structures where the expansion of ~ 0.0025 nm well exceeded the increase measured in the reacted case, other effects must be acting. Residual stresses may exist from the CTE mismatch (Fig. 1) that exists between TiB_2; however these may have been relieved somewhat by producing dislocations near TiB_2 particles (Fig. 7). Preliminary residual stress measurements using high-angle X-ray diffractometer methods [52] yielded values in the range of 100–200 MPa in both composite types [67]. This residual stress level produces an increase in lattice parameter of ~ 0.0003 nm, only accounting for about 10% of the expansion observed in the Ni_3Al-based composites. Although the same residual stress levels were detected, it is surprising that lattice dilation was measured only in the Ni_3Al-composite matrices and not the NiAl-matrices.

Reviewing the values determined for monolithic Ni_3Al, Ni_3Al + B and NiAl, the average lattice parameters compare well with other lattice constant data (compiled by Khadkikar [61]) in Table XI. The lattice parameters of the Ni_3Al, Ni_3Al + B and NiAl match well with those determined by Khadkikar [61] after canning and extruding the same powder. The parameters determined for Ni_3Al were similar to that found by Noguchi *et al.* [68] but less than that reported by Aoki and Izumi [69] and Bradley *et al.* [70]. The lattice constants for NiAl are higher than those published [71], possibly due to higher oxygen content in the alloys [61].

TABLE X Lattice parameters of the nickel aluminide powders, and hot-pressed monolithics and composite matrices

Materials	Lattice parameters (nm)		
	Powders	Monolithics[a]	Composite Matrices[a]
NiAl (B2) (Ni–45 at. % Al)	0.288 33 ± 0.0003	0.288 14 ± 0.000 02	0.288 27 ± 0.000 04
Ni_3Al (Ll_2) (Ni–24 at % Al)	0.356 91 ± 0.000 02	0.356 95 ± 0.000 01	0.359 55 ± 0.000 01
Ni_3Al + B (Ll_2) (Ni–24 at % Al–0.2 at % B)		0.357 29 ± 0.000 02	0.359 40 ± 0.000 02

[a] Samples were annealed at 873 K for 3.5 h prior to X-ray diffraction analysis.

3.4. Other studies of TiB_2 in nickel aluminide matrices

The results obtained in this investigation are consistent with conclusions drawn from other work which incorporated TiB_2 in Ni_3Al or NiAl. The only case where extensive reaction occurred between Ni_3Al and

TABLE XI Comparison of monolithic lattice parameters from the literature. Compositions are expressed in at %

Investigator	Monolithic lattice parameter (nm)		
	Ni_3Al	Ni_3Al + B	NiAl
Current study; hot-pressed powder	0.356 95 (23 Al)	0.357 29 (23 Al, 0.05B)	0.288 14 (45 Al)
Khadkikar [61]; hot extruded powder	0.356 77 (23 Al)	0.357 58 (23.8 Al; 0.02B)	0.288 34 (45 Al)
Aoki and Izumi; cast [69]	0.356 00 (24 Al)	–	–
Noguchi *et al.* [68]; cast	0.357 0 (25 Al) 0.357 4 (25 Al)	–	–
Huang *et al.* [62] ; melt-spun ribbon	0.356 77 (25 Al)	0.357 25 (24 Al, 0.05 B) 0.357 40 (25 Al, 0.05 B)	–
Bradley and Taylor [70] cast;	0.358 17 (25 Al) 0.357 44 (23.4 Al)	–	–
Taylor and Doyle [71] cast;	–	–	0.286 37 (44.7 Al) 0.286 52 (45.2 Al) 0.286 72 (46.0 Al)

TiB_2 was observed during RHP. Temperatures as high as 1823 K maintained for as long as 2 h produced an intergranular boride τ-phase in the structure [72]. The high reaction temperatures experienced and the incipient liquid phase present during processing were believed to be responsible for the reaction product. In another study involving solid-state VHP, after 25 h at 1373 K, a 10–20 μm reaction zone developed on the Ni_3Al (IC-221) side of the interface [19]. EDAX and X-ray line scans showed evidence of titanium diffusion into the matrix, zirconium accumulation at the interface, chromium precipitation in the matrix and at the interfaces, zirconium-rich precipitates in TiB_2, an absence of nickel and aluminium in the reinforcement. Only a slight reaction was detected in this case.

Limited experimental processes have consolidated composites of NiAl and TiB_2. TEM investigations of XD™ processed material has given evidence that no reactions took place [37, 73] to at least 1773 K. Bech and Lipsitt [74] on this system also confirmed the long-term chemical stability of this system (TiB_2 in Ni–51.3 at % Al, NiAl), as after exposure at 1473 K for 1000 h the boundaries remained sharp and distinct. Stoichiometric NiAl containing 15 vol % TiB_2 were processed by HIPing at 1562 K for 4 h at 103 MPa and then subsequently aged for different times at 1373 and 1473 K [75]. TEM investigations did not reveal any reaction after processing nor after 6 weeks ageing at the annealing temperatures. Investigators who reaction processed (RHIP) stoichiometric NiAl matrix composites at 1473 K for 1 h also did not note any reaction to take place.

4. Conclusions

This investigation briefly reviewed results of previous studies concerning the stability of ceramic reinforcement materials in nickel aluminide matrices. Thermodynamic analyses of interactions between TiB_2 reinforcement and NiAl (45 at % Al) or Ni_3Al (24 at % Al) matrices predicted stability at temperatures between 1173 and 1573 K. Calculations showed that no binary reaction products could form; however, slight dissolution of titanium and boron from the reinforcement in the matrices was found to be possible. Greater dissolution of titanium and boron was predicted in Ni_3Al compared to NiAl and with increase in temperature. The experimental findings from energy dispersive X-ray analyses (EDAX), Auger electron spectroscopy (AES) line scans and transmission electron microscopy (TEM) imaging of interfacial regions were consistent with the thermodynamic calculations. No distinct product phase was observed (SEM, TEM) at interfaces in either composite, although titanium and boron were detected (EDAX, AES) in the Ni_3Al matrix at levels greater than that found in the NiAl matrix. X-ray diffraction techniques did not detect reaction products in the two as-hot-pressed composites. NiAl matrix lattice parameters remained unchanged from the powder to monolithic to the composite matrix structure. Slight expansion of the Ni_3Al matrix lattice was measured after hot-pressing with TiB_2, resulting primarily from titanium diffusion from TiB_2 into the matrix. The higher activity of nickel in Ni_3Al promotes this greater instability, as shown in the thermodynamic calculations.

Acknowledgements

The authors thank NASA Lewis Research Center for partial experimental support of this work in its early stages. Primary support for the authors and the experimental portions from AFSOR 89-0508 and MTS Systems Corporation is gratefully acknowledged. The help of R. W. Margevicius and K. J. McClellan with the TEM is appreciated.

References

1. R. R. BOWMAN, R. D. NOEBE and R. DAROLIA "HITEMP Review"; NASA CP 10039, 47–1 (1989).
2. K. AOKI and O. IZUMI, *J. Jpn Inst. Metals* **43** (1979) 1190.
3. C. T. LIU, C. L. WHITE and J. A. HORTON, *Acta Metall.* **33** (1985) 213.
4. S. V. RAJ, R. D. NOEBE and R. BOWMAN, *Scripta Metall.* **23** (1989) 2049.
5. P. NAGPAL and I. BAKER, *ibid.* **24** (1990) 2381.
6. E. M. SCHULSON and D. R. BARKER, *ibid.* **17**, (1983) 519.
7. J. D. RIGNEY and J. J. LEWANDOWSKI, *Mater. Sci. Engng* **A149** (1992) 143.
8. J. M. YANG, W. H. KAO and C. T. LIU, *ibid.* **A107** (1989) 81.
9. N. S. STOLOFF and B. MOORE, "Advances in Fracture Research", Vol. 4 (Pergamon Press, New York, 1989) p. 3039.
10. J. D. RIGNEY, MS thesis, Department of Materials Science and Engineering, Case Western Reserve University, Cleveland, OH (1990).
11. J. D. RIGNEY and J. J. LEWANDOWSKI, *Mater. Sci. Engng*, (1992) **A158** (1992) 31.
12. *idem, ibid.* (1993) in preparation.
13. C. G. McKAMEY and C. A. CARMICHAEL, in "High Temperature Ordered Intermetallic Alloys IV", Materials Research Society Symposium Proceedings, edited by J. O. Stieger, L. Johnson and D. P. Pope (Materials Research Society, Pittsburgh, PA 1991) p. 1051.
14. R. M. GERMAN, A. BOSE and N. S. STOLOFF, in "High Temperature Ordered Intermetallic Alloys III", Materials Research Society, Symposium Proceedings, edited by C. T. Liu, A. I. Taub, N. S. Stoloff and C. C. Koch (Materials Research Society, Pittsburgh, PA, 1989) p. 403.
15. A. BOSE, B. MOORE. R. M. GERMAN and N. S. STOLOFF, *J. Metals* **40** (1988) 14.
16. B. MOORE, A. BOSE, R. M. GERMAN and N. S. STOLOFF, *Mater. Res. Soc. Symp. Proc.* **120**, (1988) 51
17. R. M. GERMAN and A. BOSE, *Mater. Sci. Engng* **A107** (1989) 107.
18. C. G. McKAMEY, G. L. POVRIK, J. A. HORTON, T. N. TIEGS and E. K. OHRINER, in "High Temperature Ordered Intermetallic Alloys III," Materials, Research Society Symposium Proceedings, edited by C. T. Liu, A. I. Taub, N. S. Stoloff and C. C. Koch (Materials Research Society, Pittsburgh, PA (1989) p. 609.
19. P. C. BRENNAN, W. H. KAO, S. M. JENG and J. M. YANG, ASM/TMS Fall Meeting (1989).
20. P. C. BRENNAN, W. H. KAO, H. A. KATZMAN and J-M. YANG, *J. Mater. Res.* **6** (1991) 355.
21. J. S. C. WANG, S. G. DONNELLY, P. GODAVARTI and C. C. KOCH, *Int. J. Powder Metall.* **24** (1988) 315.
22. J. M. YANG, W. H. KAO and C. T. LIU, *Metall. Trans.* **20A** (1989) 2459.
23. T. G. NIEH, J. J. STEPHENS, J. WADSWORTH and C. T. LIU in "Interfaces in Polymer, Ceramic and Metal Matrix Composites", edited by H. Ishida, (Elsevier, New York, 1988) p. 215.

24. A. BOSE B. MOORE, N. S. STOLOFF and R. M. GERMAN, in "Proceedings of the Conference on P/M Aerospace Materials", Luzern, Switzerland (1987) *J. Metals*, **40** (1988) 14.
25. P. C. BRENNAN, W. H. KAO, S. M. JENG and J. M. YANG, in "Intermetallic Matrix Composites," Materials Research Society Symposium Proceedings, Vol. 196 (1990) p. 169.
26. J. M. YANG, W. H. KAO and C. T. LIU, in "Ordered Intermetallic Alloys III", Materials Research Society Symposium Proceedings, Vol. 133, edited by C. T. Liu, A. I. Taub, N. S. Stoloff and C. C. Kock (Materials Research Society, Pittsburgh, PA, 1989) p. 453.
27. T. C. CHOU, *Scripta Metall.* **24** (1990) 409.
28. T. C. CHOU and T. G. NIEH, *J. Mater. Res.* **5** (1990) 1985.
29. R. L. MEHAN, M. R. JACKSON and M. D. McCONNELL, *J. Mater. Sci.* **18** (1983) 3195.
30. J. A. CORNIE, NASA Cr-134956 (1977).
31. G. E. FUCHS and W. H. KAO, "International P/M Conference", American Powder Metallurgy Institute, Orlando, FL (1988).
32. G. E. FUCHS, "High-Temperature Ordered Intermetallic Alloys III", Materials Research Society Symposium proceedings, Vol. 133, edited by C. T. Liu, A. I. Taub, N. S. Stoloff and C. C. Koch (Materials Research Society, Pittsburgh, PA 1989) p. 615.
33. S. M. PIERIK, D. R. BARKER and M. J. KAUFMAN, ASM/*TMS Fall Meeting* (1989).
34. R. BOWMAN and R. D. NOEBE, *Adv. Mater. Processes.* **8** (1989) 35.
35. T. C. CHOU and T. G. NIEH, *Scripta Metall.* **25** (1991) 2059
36. D. M. SHAH, C. W. MUSSON and D.L. ANTON, United Technologies Interim Technical Report, FR 20410-5 (1989).
37. K. S. KUMAR, S. K. MANNAN, J. D. WHITTENBERGER, R.K. WISWANADAN and L. CHRISTODOULU, Martin Marietta Laboratories, Report no. MMLTR 89-102(c) (1989).
38. R. R. BOWMAN, R. D. NOEBE and M. V. NATHAL, "HITEMP Review"; NASA CP 10039, 54–1 (1989).
39. A. J. CARBONE, M. W. KOPP, J. K. TIEN, S. S. LIU, H. L. MARCUS and S. L. DRAPER, *Scripta Metall.* **22** (1988) 1903.
40. A. K. MISRA, *Metall. Trans.* **22A** (1991) 2535
41. *idem, NASA, CR*-4171 (1988).
42. R. W. BARTLETT, J. W. McCAMONT and P. R. GAGE, *J. Amer. Ceram. Soc.* **48** (1965) 551.
43. E. V. CLOUGHERTY, R. L. POBER and L. KAUFMAN, Trans. Met. Soc. AIME **246** (1968) 1077.
44. R. J. IRVING and I. G. WORSLEY. *J. Less-Common Metals.* **16** (1968) 103.
45. A. K. KURIAKOSE and J. L. MARGROVE, *J. Electrochem. Soc.* **111** (1976) 827.
46. L. KAUFMAN and E. V. CLOUGHERTY, in "Metals for the Space Age", Plansee Proceedings, edited by F. Benesovsky (MetallWerk Plansee Ges. m.b.h Reutte, Austria, 1965).
47. J. R. RAMBERG and W. S. WILLIAMS, *J. Mater. Sci.* **22** (1987) 1815.
48. Y. S. TOULOUKIAN, R. K. KIRBY, R. E. TAYLOR and P. H. DESAI, "Thermophysical Properties of Matter", Vols. 12 and 13 (Plenum, New York, 1977).
49. C. T. LYNCH, S. A. MERSOL and S. W. VAHLDIEK, *J. Less-Common Metals* **10** (1966) 206.
50. W. J. LEOBRUNO, J. S. HAGGERTY and J. L. O'BRIEN, *Mater Res. Soc. Bull.* **3** (1968) 361.
51. S. G. KEIHN and J. KEPLIN *J. Amer. Ceram. Soc.* **50** (1967) 81.
52. B. D. CULLITY, "Elements of X-Ray Diffraction" (Addison-Wesley, Reading, MA 1978) p. 363.
53. A. K. MISRA, *Metall. Trans.* **21A** (1990) 441.
54. M. F. SINGLETON, J. L. MURRAY and P. NASH in "Binary Alloy Phase Diagrams", Vol. 1, edited by T.B. Massalski, (American Society for Metals, Metals Park, OH, 1986), p. 146.
55. A. STEINER and L. KOMAREK, *Trans. Met. Soc. AIME* **230** (1964) 786.
56. R. E. HANNEMAN and A. U. SEYBOLT, *ibid.* **245** (1969) 434.
57. D. BERNIE, E. S. MACHLIN, L. KAUFMAN and K. TAYLOR, *CALPHAD* **6** (1982) 93.
58. L. KAUFMAN and R. NESOR, *ibid.* **2**, (1978) 81.
59. *idem, ibid.* **2** (1978) 325.
60. P. G. NASH, *Bull. Alloy Phase Diag.* **3** (1982) 367.
61. P. S. KHADKIKAR, PhD dissertation, Department of Materials Science and Engineering, Case Western Reserve University, Cleveland OH (1988).
62. S. C. HUANG, A. I. TAUB, K. M. CHANG, *Acta Metall.* **32** (1984) 1703.
63. S. OCHIAI, Y. MISHIMA and T. SUZUKI, *Bull. PME (TIT)* **53** (1984) 15.
64. M. P. ARBUZOV and I. A. ZELENOV, *Fiz. Met. Metalloved* **15** (1963) 725.
65. R. W. GUARD and J. H. WESTBROOK, *Trans. Met. Soc. AIME*, **215** (1959) 807.
66. W. B. PEARSON, "A Handbook of Lattice Spacing and Structures of Metals and Alloys" Vol. 2 (Pergamon Press, New York, 1968).
67. J. D. RIGNEY, unpublished results 1992.
68. O. NOGUCHI, Y. OYA and T. SUZUKI, *Metall. Trans.* **12A** (1981) 1647.
69. K. AOKI and O. IZUMI, *Phys. Status, Solidi (a)* **32** (1975) 657.
70. A. J. BRADLEY and A. TAYLOR. *Proc. Roy. Soc.* **A136** (1937) 210.
71. A. TAYLOR and N. J. DOYLE, *J. Appl. Crystallogr.* **5** (1972) 201.
72. P. ANGELINE, P. F. BECHER , J. BENTLEY, C. B. FINCH and P. S. SKLAD in "Defect Properties and Processing of High Technology Non-metallic Materials", edited by J.H. Crawford, Y. Chen and W. A. Sibley Vol. (MRS Pittsburgh, PA 1984) p. 299.
73. L. WANG and R. J. ARSENAULT, *Metall. Trans.* **22A**, (1991) 3013.
74. H. BECH and H. A. LIPSITT, ASM/TMS Fall Meeting (1989).
75. M. SAQIB, G. M. MEHROTOTRA, I. WEISS, H. BECH and H. A. LIPSITT, *Scripta Metall.* **24** (1990) 1889.

Received 20 July 1992
and accepted 4 January 1993.